SKIN-EFFECT INFLUENCE ON THREE-DIMENSIONAL INSTABILITY OF A TRAVELING MAGNETIC FIELD DRIVEN FLOW IN A CYLINDRICAL CONTAINER

A. Yu. Gelfgat, E. Kit

School of Mechanical Engineering, Faculty of Engineering, Tel-Aviv University, Ramat Aviv, Tel-Aviv 69978, Israel (gelfgat@eng.tau.ac.il)

Introduction. The traveling magnetic field (TMF) is one of various MHD tools used for the electromagnetic control of melt flows in bulk semiconductor crystal growth [1]–[3]. Conversely to the widely used rotating magnetic field (RMF) the traveling magnetic field yields a possibility to create or control meridional melt circulations directly, i.e., without unnecessary inducing of a non-uniform rotational flow. This possibility initiated a number of recent studies devoted to the TMF-driven and TMF-controlled flows regarding various crystal growth applications in terrestrial and microgravity environment (see [1]–[7] and references therein).

One of the important problems directly connected with the TMF driving and control of melt flows in crystal growth processes is the stability of the resulting time-average flow. The study of this issue was started in [4], where the simplest possible expression for TMF driving forces was used. The model considered in [4] corresponds to small dimensionless TMF wavenumbers α and small dimensionless circular frequency γ, and does not account for a possible skin-effect. The present study extends results of [4] to the cases of moderate and large wavenumbers. The TMF driven flow in a cylindrical container is considered. In the following we discuss how the time-averaged TMF force and the TMF-driven flow patterns change with the growth of TMF wavenumber and TMF frequency. Then we study the three-dimensional stability of axisymmetric TMF-driven flows for different aspect ratios of the container and the TMF wavenumber and dimensionless frequency varying independently from 1 to 20. The calculations are performed using the global Galerkin method described in [8].

With the increase of the TMF wavenumber the time-averaged TMF driving force exhibits a significant skin-effect. We study how the flow varies with the TMF wavenumber and show that intensity of the TMF-induced vortex grows rapidly with the increase of the TMF wavenumber from a small value $\alpha < 1$ to a moderate value $1 < \alpha < 10$, which depends on the aspect ratio and the TMF force amplitude. With further increase of α the intensity slowly decreases. A similar change of the flow intensity is observed when the parameter γ is varied in the interval $1 \le \gamma \le 20$.

The present study shows that the dependence of the stability properties of the flow on the TMF wavenumber and the skin depth is rather complicated. The details are given in [7]. The marginal stability curves contain non-monotonic parts with turning points and reinstatement of stability. Generally, the critical amplitude of the electromagnetic force steeply reduces with the increase of α or γ from the value $\alpha = 1$ ($\gamma = 1$) and then slowly increases for $\alpha > 10$ ($\gamma > 10$), thus behaves correspondingly to the increase or decrease of the intensity of the main TMF-induced vortex. The patterns of the most unstable perturbations show that the transition from an axisymmetric to the three-dimensional flow should be attributed to the instability of the main vortex and not to the thin skin-layer, even for large values of α or γ.

1. Formulation of the problem. We consider a flow of a Newtonian incompressible electrically conducting fluid in a cylindrical enclosure $0 \le r \le R$, $0 \le z \le H$ under action of a magnetic field traveling along the z-axis. It is assumed that at the cylindrical sidewall the vector potential of the magnetic field is given by

$$A_r = 0, \quad A_\theta = A_0 \mathrm{e}^{i(\omega t - \tilde{\alpha} z)}, \quad A_z = 0\,, \tag{1}$$

where $\tilde{\alpha}$ and ω are the wavenumber and the circular frequency of the traveling magnetic field.

Assuming that magnetic Reynolds number is small the effect of the fluid flow on the magnetic field is neglected. Additionally, we assume that the flow is decomposed into time-averaged and oscillating parts and that the amplitude of the oscillating part is much smaller than that of the average part. This assumption is justified for large frequency of the magnetic field, which usually is about 50 Hz or even larger. Under the assumptions made the time-averaged part of the flow is driven by a time-averaged electromagnetic force $\mathbf{f}$ and is described by the dimensionless momentum and continuity equations

$$\frac{\partial \mathbf{v}}{\partial t} + (\mathbf{v} \cdot \nabla)\, \mathbf{v} = -\nabla p + \Delta \mathbf{v} + \mathbf{f}, \qquad \nabla \cdot \mathbf{v} = 0\,, \tag{2)(3}$$

where $\mathbf{v}$ is the fluid velocity and p is the pressure. The scales of length, time, velocity and pressure are R, R^2/ν, ν/R and $\rho\nu^2/R^2$, respectively, where ρ is the fluid density and ν is the kinematic viscosity.

The expression for the electromagnetic force $\mathbf{f}$ depends on a configuration of a magnetic field inductor. In the case of an infinite cylinder in an infinite inductor the problem for the magnetic and electric fields allows for an analytical solution, which yields the following expression for the time-averaged electromagnetic force [5]:

$$f_r = -Ft \frac{Im\left[I_1\left(\beta^* r\right) I_0\left(\beta r\right)\right]}{\left|I_0\left(\beta\right)\right|^2}, \qquad f_\theta = 0, \qquad f_z = Ft\alpha \frac{\left|I_1\left(\beta r\right)\right|^2}{\left|I_0\left(\beta\right)\right|^2} \tag{4}$$

Here $Ft = A_0^2 \omega \sigma R^2 / 2\rho\nu^2$, $\alpha = \tilde{\alpha} R$, $\beta = \sqrt{\alpha^2 + i\gamma}$, $\gamma = \sigma\omega\mu R^2$, and μ is the magnetic permeability. An additional parameter defining the flow is the aspect ratio of the cylinder $A = H/R$. More complicated expressions, which take into account the finite extent of the inductor and the cylinder, as well as the distance between them, were obtained recently in [6]. It should be noticed that the radial component of the electromagnetic force (4) is potential and therefore does not affect the flow velocity. However, it is not small compared to the axial component and should be taken into account if correct pressure distribution is needed.

The value of dimensionless wavenumber is equal to $\alpha = 2\pi R/L$, where L is the TMF wavelength. At large L the wavenumber tends to zero. Assuming additionally that the dimensionless TMF frequency gamma is also small the expression for the z-component of the electromagnetic force (4) can be approximated asymptotically as

$$f_z = Ft\alpha \left|\beta\right|^2 \frac{r^2}{4} = Fb \frac{r^2}{4}, \qquad Fb = B_0^2 \frac{\omega\sigma\tilde{\alpha} R^5}{2\rho\nu^2} \tag{5}$$

This expression was used for the stability analysis in [4]. In Fig. 1 we compare the force f_z for $\gamma = 1$ and different α using expressions (4) and (5). It is seen that Eq. (5) gives a good approximation only for $\alpha < 1$ and $\gamma < 1$. Equations (4) must be accounted for already at $\alpha = 2$. For $\alpha > 3$ the force is characterized by a rapid growth near the cylinder wall ($r = 1$), i.e., the well-known skin-effect is observed.

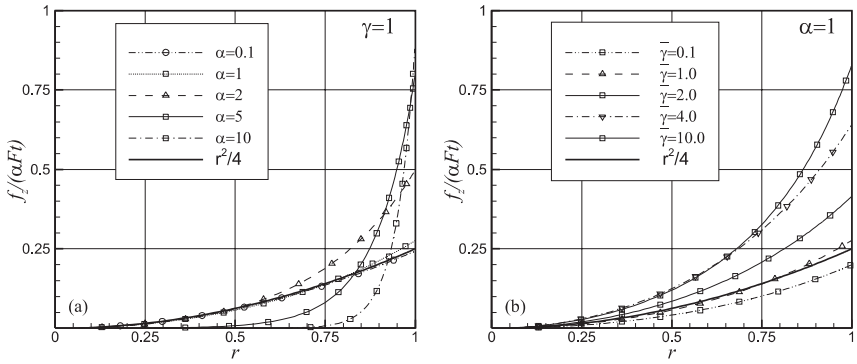

Fig. 1. Dependence of the time-averaged electromagnetic force on the parameters α and γ.

Assuming that the TMF wavelength is of the order of the cylinder radius the value of α can be estimated as 2π, and exceeds ten for $L < R/2$. In our calculations we consider $1 \le \alpha \le 20$, and $1 \le \gamma \le 20$, which allows us to study the influence of the skin-effect on both flow patterns and their stability. For $\alpha < 1$ and $\gamma < 1$ results of [4] apply. As in [4] we consider the no-slip boundary conditions on all the borders.

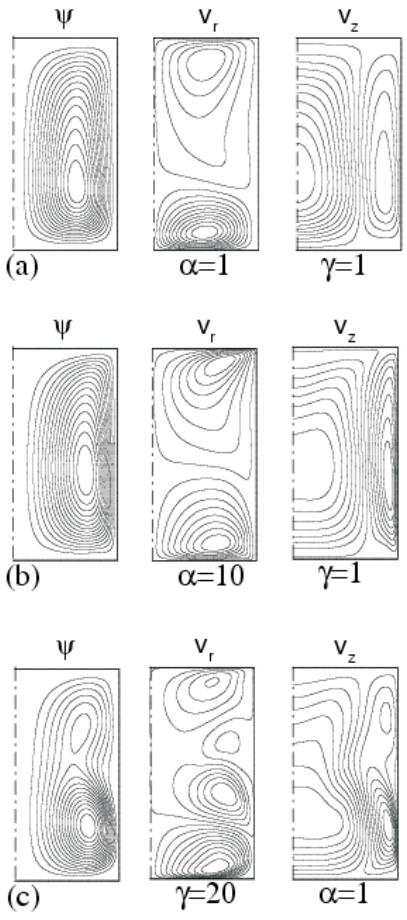

Fig. 2. Flow patterns for $A = 2$, $Ft = 10^5$.

2. Results and conclusions. The details on the steady axisymmetric flow patterns and the stability results are given in [7]. They can be summarized as follows.

With the increase of α or γ from a small value the flow intensity increases. Beyond $\alpha \approx 6$ and $\gamma \approx 7$ the intensity slowly decreases. This is illustrated in Table 1 for the growing value of α. Examples of the calculated flow patterns are shown in Fig. 2. In all the figures the flow rises along the cylindrical sidewall and then descends along the axis.

The stability diagrams corresponding to the onset of three-dimensional instability with respect to the perturbations represented as $a(r,z)\exp\left[i(k\theta + \lambda t)\right]$ were computed for the aspect ratios of the cylinder $H/R = 1$, 2, 3 and 4. Examples of the stability diagrams are given in Figs. 3 and 4.

The calculated dependencies $Ft_{\rm cr}(\alpha)$ and $Ft_{\rm cr}(\gamma)$ are not always smooth and sometimes can contain turning points and reinstatement of stability, so that the axisymmetric base flow can become unstable at $Ft_{\rm cr}^{(1)}$, then stable at $Ft_{\rm cr}^{(2)} > Ft_{\rm cr}^{(1)}$, and finally unstable at $Ft_{\rm cr}^{(3)} > Ft_{\rm cr}^{(2)}$. This can lead to a complicated dynamics in the supercritical regimes and should be taken into account

Table 1. Maximal and minimal values of ψ, v_r and v_z for $A = 2$, $\gamma = 1$, and $Ft = 10^5$.

	$\alpha = 1$	$\alpha = 2$	$\alpha = 4$	$\alpha = 6$	$\alpha = 8$	$\alpha = 10$
$\psi_{\min}$	-25.78	65.143	-123.37	-143.63	-148.52	-147.50
$v_{r\min}$	-53.702	-214.39	-480.62	-562.16	-563.66	-532.61
$v_{r\max}$	143.45	318.51	558.00	638.21	639.99	602.91
$v_{z\min}$	-189.95	-361.84	-659.65	-776.94	-813.53	-819.93
$v_{z\max}$	155.36	414.83	800.58	949.85	1005.1	1017.7

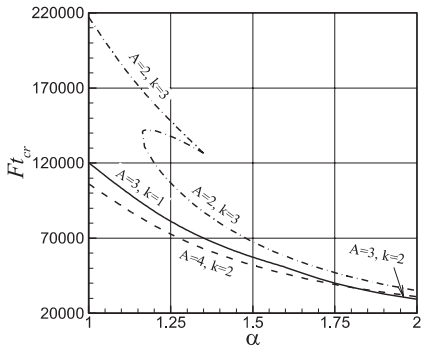

Fig. 3. Critical curves for $A = 2$ and 4; $\alpha = 1$, $1 < \gamma < 2$.

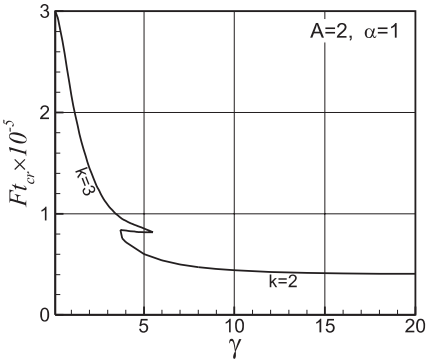

Fig. 4. Critical curve for $A = 2$, $\alpha = 1$.

if time-dependent calculations are performed. On the basis of the patterns of the most unstable three-dimensional perturbations it was concluded that the transition from an axisymmetric to a three-dimensional flow state takes place due to instability of the whole TMF-induced vortex, and not due to disturbances developing in the skin-layer.

Acknowledgement. This study was supported by the German-Israeli Foundation, grant No. 1-794-145.10/2004.

REFERENCES

1. Yu. Gelfgat, J. Krūmiņš, M. Abricka. Motion of an electrically conducting fluid in a cylindrical volume exposed to the influence of superimposed rotating and magnetic field. *Magnetohydrodynamics*, vol. 36 (1999), no. 1, pp. 3–16.
2. N. Ramachandran, K. Mazuruk, M.P. Volz. Use of traveling magnetic fields to control melt convection. *SPIE*, vol. 3792 (1999), pp. 39–47.
3. M. Abricka, Yu. Gelfgat, J. Krūmiņš. Influence of combined electromagnetic fields on the heat/mass transfer in the Bridgman process. *Energy Conversion and Management*, vol. 43 (2002), pp. 327–333.
4. I. Grants, G. Gerbeth. Stability of melt flow due to a traveling magnetic field in a closed ampoule. *J. Cryst. Growth*, vol. 269 (2004), pp. 630–638.
5. J. Krūmiņš. *Fundamentals of theory and calculation for devices with a traveling magnetic field* (Zinātne Publishing House, Riga, 1983). (in Russ).
6. M.P. Volz, K. Mazuruk. Lorenz body force induced by traveling magnetic fields. *Magnetohydrodynamics*, vol. 40 (2004), no. 2, pp. 117–126.
7. A.Yu. Gelfgat. On three-dimensional instability of a traveling magnetic field driven flow in a cylindrical container. *J. Cryst. Growth*, (to appear).
8. A.Yu. Gelfgat. Two- and three-dimensional instabilities of confined flows: numerical study by a global Galerkin method. *CFD Journal*, vol. 9 (2001), pp. 437–448.